Precipitation changes in the Mediterranean basin during the Holocene from terrestrial and marine pollen records: A model/data comparison

Odile Peyron[1], Nathalie Combourieu-Nebout[2], David Brayshaw[3], Simon Goring[4], Valérie Andrieu-Ponel[5], Stéphanie Desprat[6,7], Will Fletcher[8], Belinda Gambin[9], Chryssanthi Ioakim[10], Sébastien Joannin[1], Ulrich Kotthoff[11], Katerina Kouli[12], Vincent Montade[1], Jörg Pross[13], Laura Sadori[14], Michel Magny[15]

[1] Institut des Sciences de l'Evolution (ISEM), Université de Montpellier, France

[2] UMR 7194 MNHN, Institut de Paléontologie Humaine 1, Paris, France

[3] University of Reading, Department of Meteorology, United Kingdom

[4] Department of Geography, Univ. of Wisconsin-Madison, Wisconsin, USA

[5] Institut Méditerranéen de Biodiversité et d'Ecologie marine et continentale (IMBE), Aix Marseille Université, Aix-en-Provence, France

[6] EPHE, PSL Research University, Laboratoire Paléoclimatologie et Paléoenvironnements Marins, Pessac, France

[7] Univ. Bordeaux, EPOC UMR 5805, Pessac, France

[8] Geography, School of Environment, Education and Development, University of Manchester, United Kingdom

[9] Institute of Earth Systems, University of Malta, Malta

[10] Institute of Geology and Mineral Exploration, Athens, Greece

[11] Center for Natural History and Institute of Geology, Hamburg University, Hamburg, Germany

[12] Department of Geology and Geoenvironment, National and Kapodistrian University of Athens, Greece

[13] Paleoenvironmental Dynamics Group, Institute of Earth Sciences, Heidelberg University, Germany

[14] Dipartimento di Biologia Ambientale, Università di Roma "La Sapienza", Roma, Italy

[15] UMR 6249 Chrono-Environnement, Université de Franche-Comté, Besançon, France

Correspondence to: O. Peyron (odile.peyron@univ-montp2.fr)

28   Abstract

29   Climate evolution of the Mediterranean region during the Holocene exhibits strong spatial and

30   temporal variability. The spatial differentiation and temporal variability, as evident from

31   different climate proxy datasets, has remained notoriously difficult for models to reproduce. In

32   light of this complexity, we propose here a new paleo-observations synthesis and its comparison

33   – at regional/local level – with a climate model data to examine (i) opposing northern and

34   southern precipitation regimes during the Holocene across the Mediterranean basin, and (ii) an

35   east-to-west precipitation dipole during the early Holocene, from a wet eastern Mediterranean

36   to dry western Mediterranean. Using precipitation estimates inferred from marine and terrestrial

37   pollen archives, we focus on two key time intervals, the early to mid-Holocene (8000 to 6000

38   cal yrs BP) and the late Holocene (4000 to 2000 yrs BP), in order to test the above mentioned

39   hypotheses on a Mediterranean-wide scale, and we compare the results with model outputs from

40   a high-resolution regional climate model. Spatially, we focus on transects across the

41   Mediterranean basin from north to south and from west to east. Because seasonality represents

42   a key parameter in Mediterranean climates, special attention was given to the reconstruction of

43   season-specific climate information, notably summer and winter precipitation. The

44   reconstructed climatic trends corroborate a previously described north-south partition of

45   precipitation regimes during the Holocene, but more sites from the northern part of the

46   Mediterranean basin are needed to further substantiate these observations. During the early

47   Holocene, relatively wet conditions occurred in the south-central and eastern Mediterranean

48   region, while drier conditions prevailed from 45°N northwards. These patterns then appear to

49   reverse during the late Holocene, with similar to present day or slightly drier than present day

50   conditions in the south-central region. With regard to the existence of a west-east precipitation

51   dipole during the Holocene, our pollen-based climate data show that the strength of this dipole

52   is strongly linked to the seasonal parameter reconstructed; early Holocene summers show a

53   clear east-west division, with summer precipitation having been highest in Greece and the

54   eastern Mediterranean and lowest over the Italy and the western Mediterranean. Summer

55   precipitation in the east remained above modern values, even during the late Holocene interval.

56   In contrast, winter precipitation signals are less spatially coherent during the early Holocene

57   but low precipitation is evidenced during the late Holocene. A general drying trend occurred

58   from the early to the late Holocene, particularly in the central and eastern Mediterranean.

59   For the same time intervals, site-based pollen-inferred precipitation estimates were compared

60   with model outputs, more specifically with an existing database from a regional-scale

61   downscaling (HadRM3) of a set of global climate-model simulations (HadAM3). The high-
62   resolution detail achieved through the downscaling is intended to enable a better comparison
63   between 'site-based' paleo-reconstructions and gridded model data in the complex terrain of
64   the Mediterranean; the climate model outputs and pollen-inferred precipitation estimates show
65   some overall correspondence, though modeled changes are extremely small and at the absolute
66   margins of statistical significance. There are suggestions that the eastern Mediterranean
67   experienced wetter than present summer conditions during the early and late Holocene; the
68   drying trend in winter from the early to the late Holocene also appears to be simulated. Although
69   some simulated patterns are of marginal statistical significance at the large scale, the use of this
70   high-resolution regional climate model highlights how the inherently "patchy" nature of climate
71   signals and palaeo-records in the Mediterranean basin may lead to local signals much stronger
72   than the large-scale pattern would suggest. Nevertheless, the east to west division in summer
73   precipitation seems more marked in the pollen reconstruction than in the model outputs. The
74   footprint of the anomalies (like today or dry winters, wet summers) has some similarities to
75   modern analogue atmospheric circulation patterns associated with a strong westerly circulation
76   in winter (positive AO/NAO) and a weak westerly circulation in summer associated with anti-
77   cyclonic blocking; although there also remain important differences between the palaeo-
78   simulations and these analogues. The regional climate model, consistent with other global
79   models, does not suggest an extension of the African summer monsoon into the Mediterranean;
80   so the extent to which summer monsoonal precipitation may have existed in the southern and
81   eastern Mediterranean during the mid-Holocene remains an outstanding question.

82
83

1   Introduction

The Mediterranean region is particularly sensitive to climate change due to its position within the confluence of arid North African (i.e. subtropically influenced) and temperate/humid European (i.e. mid-latitudinal) climates (Lionello, 2012). Palaeoclimatic proxies, including stable isotopes, lipid biomarkers, palynological data and lake-levels, have shown that the Mediterranean region experienced climatic conditions that varied spatially and temporally throughout the Holocene (e.g. Bar-Matthews and Ayalon, 2011; Luterbacher et al., 2012; Lionello, 2012; Triantaphyllou et al., 2014, 2016; Mauri et al., 2015; De Santis and Caldara 2015; Sadori et al., 2016a) and well before (eg. Sadori et al., 2016b). Clear spatial climate patterns have been identified from east to west and from north to south within the basin (e.g. Zanchetta et al., 2007; Magny et al., 2009b, 2011, 2013; Zhornyak et al., 2011; Sadori et al., 2013; Fletcher et al., 2013). Lake-level reconstructions from Italy thus suggest contrasting patterns of palaeohydrological changes for the central Mediterranean during the Holocene (Magny et al., 2012, 2013). Specifically, lake level maxima occurred south of approximately 40°N in the early to mid-Holocene, while lakes north of 40°N recorded minima. This pattern was reversed at around 4500 cal yrs BP (Magny et al., 2013). Quantitative pollen-based precipitation reconstructions from sites in northern Italy indicate humid winters and dry summers during the early to mid-Holocene, whereas southern Italy was characterised by humid winters and summers; the N-S pattern reverses in the late Holocene, with drier conditions at southern sites and wet conditions at northern sites (Peyron et al., 2011, 2013). These findings support a north–south partition for the central Mediterranean with regards to precipitation, and also confirm that precipitation seasonality is a key parameter in the evolution of Mediterranean climates. The pattern of shifting N-S precipitation regimes has also been identified for the Aegean Sea (Peyron et al., 2013). Taken together, the evidence from pollen data and from other proxies covering the Mediterranean region suggest a climate response that can be linked to a combination of orbital, ice-sheet and solar forcings (Magny et al., 2013).

An east-west pattern of climatic change during the Holocene is also suggested in the Mediterranean region (e.g. Combourieu Nebout et al., 1998; Geraga et al., 2010; Colmenero-Hildago et al., 2002; Kotthoff et al., 2008; Dormoy et al., 2009; Finne et al., 2011; Roberts et al., 2011, 2012; Luterbacher et al., 2012; Guiot and Kaniewski, 2015). An east-west division during the Holocene is observed from marine and terrestrial pollen records (Dormoy et al., 2009; Guiot and Kaniewski, 2015), lake-level reconstructions (Magny et al., 2013) and speleothem isotopes (Roberts et al. 2011).

This study aims to reconstruct and evaluate N-S and E-W precipitations patterns for the Mediterranean basin, over two key periods in the Holocene, the early Holocene 8000-6000 cal yrs BP, corresponding to the "Holocene climate optimum" and the late Holocene 4000-2000 cal yrs BP corresponding to a trend towards drier conditions. Precipitation reconstructions are particularly important for the Mediterranean region given that precipitation rather than temperature represents the dominant controlling factor on the Mediterranean environmental system during the early to mid-Holocene (Renssen et al., 2012). Moreover, the reconstruction of precipitation parameters seems robust for the Mediterranean area (Combourieu-Nebout et al., 2009; Mauri et al., 2015; Peyron et al., 2011, 2013; Magny et al., 2013).

Precipitation is estimated for five pollen records from Greece, Italy and Malta, and for eight marine pollen records along a longitudinal gradient from the Alboran Sea to the Aegean Sea. Because precipitation seasonality is a key parameter of change during the Holocene in the Mediterranean (Rohling et al., 2002; Peyron et al., 2011; Mauri et al., 2015), the quantitative climate estimates focus on reconstructing changes in summer and winter precipitation.

Paleoclimate proxy data are essential benchmarks for model intercomparison and validation (e.g. Morrill et al., 2012; Heiri et al., 2014). This holds particularly true considering that previous model-data intercomparisons have revealed substantial difficulties for GCMs in simulating key aspects of mid-Holocene climate (Hargreaves et al., 2013) for Europe (Mauri et al., 2014), and notably for southern Europe (Davis and Brewer, 2009; Mauri et al., 2015). We also aim to identify and quantify the spatio-temporal climate patterns in the Mediterranean basin for the two key intervals of the Holocene (8000–6000 and 4000–2000 cal yrs BP) based on regional-scale climate model simulations (Brayshaw et al., 2011a). Finally, we compare our pollen-inferred climate patterns with regional-scale climate model simulations in order to critically assess the consistency of the climate reconstructions revealed by these two complimentary routes.

The first originality of our approach is that we estimate the magnitude of precipitation changes and reconstruct climatic trends across the Mediterranean using both terrestrial and marine high-resolution pollen records. The signal reconstructed is then more regional than in the studies based on terrestrial records alone. Moreover, this study aims to reconstruct precipitations patterns for the Mediterranean basin over two key periods in the Holocene while the existing large-scale quantitative paleoclimate reconstructions for the Holocene are often limited to the mid-Holocene - 6000 yrs BP- (Cheddadi et al., 1997; Bartlein et al., 2011; Mauri et al., 2014), except the climate reconstruction for Europe proposed by the study of Mauri et al. (2015).

150 The second originality of our approach is that we propose a data/model comparison based on
151 (1) two time-slices and not only the mid-Holocene, a standard benchmark time period for this
152 kind of data–model comparison; (2) a high resolution regional model (RCM) which provides a
153 better representation of local/regional processes and helps to better simulate the localized,
154 "patchy", impacts of Holocene climate change, when compared to coarser global GCMs (e.g.
155 Mauri et al., 2014); (3) changes in seasonality, particularly changes in summer atmospheric
156 circulation which have not been widely investigated (Brayshaw et al., 2011).

157

158 **2 Sites, pollen records, and models**

159 The Mediterranean region is at the confluence of continental and tropical air masses.
160 Specifically, the central and eastern Mediterranean is influenced by monsoonal systems, while
161 the north-western Mediterranean is under stronger influence from mid-latitude climate regimes
162 (Lionello et al., 2006). Mediterranean winter climates are strongly affected by storm systems
163 originating over the Atlantic. In the western Mediterranean, precipitation is predominantly
164 affected by the North Atlantic Oscillation (NAO), while several systems interact to control
165 precipitation over the northern and eastern Mediterranean (Giorgi and Lionello, 2008).
166 Mediterranean summer climates are dominated by descending high pressure systems that lead
167 to dry/hot conditions, particularly over the southern Mediterranean where climate variability is
168 strongly influenced by African and Asian monsoons (Alpert et al., 2006) with strong
169 geopotential blocking anomalies over central Europe (Giorgi and Lionello, 2008; Trigo et al.,
170 2006).

171 The palynological component of our study combines results from five terrestrial and eight
172 marine pollen records to provide broad coverage of the Mediterranean basin (Fig. 1, Table 1).
173 The terrestrial sequences comprise pollen records from lakes along a latitudinal gradient from
174 northern Italy (Lakes Ledro and Accesa) to Sicily (Lake Pergusa), one pollen record from Malta
175 (Burmarrad) and one pollen record from Greece (Tenaghi Philippon). The marine pollen
176 sequences are situated along a longitudinal gradient across the Mediterranean Sea; from the
177 Alboran Sea (ODP Site 976 and core MD95-2043), Siculo-Tunisian strait (core MD04-2797),
178 Adriatic Sea (core MD90-917), and Aegean Sea (cores SL152, MNB-3, NS14, HCM2/22). For
179 each record we used the chronologies as reported in the original publications (see Table 1 for
180 references).

181   Climate reconstructions for summer and winter precipitation (Figs. 2 and 3) inferred from the
182   terrestrial sequences and marine pollen records were performed using the Modern Analogue
183   Technique (MAT; Guiot, 1990). The MAT compares fossil pollen assemblages to modern
184   pollen assemblages with known climate parameters. The MAT is calibrated using an expanded
185   surface pollen dataset with more than 3600 surface pollen samples from various European
186   ecosystems (Peyron et al., 2013). In this dataset, 2200 samples are from the Mediterranean
187   region, and the results shows that the analogues selected here are limited to the Mediterranean
188   basin. Since the MAT uses the distance structure of the data and essentially performs local
189   fitting of the climate parameter (as the mean of *n*-closest sites), it may be less susceptible to
190   increased noise in the data set, and less likely to report spurious values than others methods (for
191   more details on the method, see Peyron et al., 2011). *Pinus* is overrepresented in marine pollen
192   samples (Heusser and Balsam, 1977; Naughton et al., 2007), and as such *Pinus* pollen was
193   removed from the assemblages (both modern and fossil) for the calibration of marine records
194   using MAT. The reliability of quantitative climate reconstructions from marine pollen records
195   has been tested using marine core-top samples from the Mediterranean in Combourieu-Nebout
196   et al. (2009), which shows an adequate consistency between the present day observed and MAT
197   estimations for annual and summer precipitations values.

198   The climate model simulations used in the model-data comparison are taken from Brayshaw et
199   al. (2010, 2011a, 2011b). The HadAM3 global atmospheric model (resolution 2.5° latitude x
200   3.75° longitude, 19 vertical levels; Pope et al., 2000) is coupled to a slab ocean (Hewitt et al.,
201   2001) and used to perform a series of time slice experiments. Each time-slice simulation
202   corresponds to 20 model years after spin up (40 model years for pre-industrial). The time slices
203   correspond to "present-day" (1960-1990), 2000 cal BP, 4000 cal BP, 6000 cal BP and 8000 cal
204   BP conditions, and are forced with appropriate insolation (associated with changes in the
205   Earth's orbit), and atmospheric CO_2 and CH_4 concentrations. The heat fluxes in the ocean are
206   held fixed using values taken from a pre-industrial control run (i.e., the ocean 'circulation' is
207   assumed to be invariant over the time-slices) and there is no sea-level change, but sea-surface
208   temperatures are allowed to evolve freely. The coarse global output from the model for each
209   time slice is downscaled over the Mediterranean region using HadRM3 (i.e. a limited area
210   version of the same atmospheric model; resolution 0.44° x 0.44°, with 19 vertical levels). Unlike
211   the global model, HadRM3 is not coupled to an ocean model; instead, sea-surface temperatures
212   are derived directly from the HadSM3 output.

213 Following Brayshaw et al. (2011a), time slice experiments are grouped into "mid Holocene"
214 (8000 BP and 6000 cal yrs BP) and "late Holocene" (4000 BP and 2000 cal yrs BP) experiments
215 because (1) these two periods are sufficiently distant in the past to be substantially different
216 from the present but close enough that the model boundary conditions are well known; (2) these
217 two periods are rich in high resolution and well-dated palaeoecological sequences, providing a
218 good spatial coverage suitable for large-scale model-data comparison. These two experiments
219 aid interpretability and increase the signal-to-noise ratio (the change in forcing between
220 adjacent time-slices is relatively small, making it difficult to detect). To aid comparison with
221 proxies, changes in climate are expressed as differences with respect to the present day (roughly
222 1960-1990) rather than the pre-industrial control run: therefore the climate anomalies shown
223 thus include a component which is attributable to anthropogenic increases in greenhouse gases
224 in the industrial period, as well as longer term 'natural' changes (e.g., orbital forcing). We
225 suggest it may be better to use 'present day' to be in closer agreement with the pollen data
226 (modern samples) which use the late 20th century long-term averages (1961-1990). However,
227 there are some quite substantial differences between model runs under 'present day' and
228 'preindustrial' forcings (Figure 4). Statistical significance is assessed with the Wilcoxon-Mann-
229 Whitney significance test (Wilks, 1995).

230 The details of the climate model simulations are discussed at length in Brayshaw et al (2010,
231 2011a, 2011b). These includes a detailed discussion of verification under present climate, the
232 model's physical/dynamical climate responses to Holocene period 'forcings', and comparison
233 to other palaeoclimate modelling approaches (e.g., PMIP projects) and palaeo-climate
234 syntheses. The GCM used (HadAM3 with a slab ocean) is comparable to the climate models in
235 PMIP2, but a key advantages of the present dataset is: (a) the inclusion of multiple time-slices
236 across the Holocene period; and (b) the additional high-resolution regional climate model
237 downscaling enables the impact of local climatic effects within larger-scale patterns of change
238 to be distinguished (e.g., the impact of complex topography or coastlines; Brayshaw et al
239 2011a), potentially allowing clearer comparisons between site-based proxy-data and model
240 output.

241

242 **3   Results and Discussion**

243

244 *A North-South precipitation pattern?*

245 Pollen evidence shows contrasting patterns of palaeohydrological changes in the central
246 Mediterranean. The early- to mid-Holocene was characterized by precipitation maxima south
247 of around 40°N while at the same time, northern Italy experienced precipitation minima; this
248 pattern reverses after 4500 cal yrs BP (Magny et al., 2012b; Peyron et al., 2013). Other proxies
249 suggest contrasting north-south hydrological patterns not only in central Mediterranean but also
250 across the Mediterranean (Magny et al., 2013), suggesting a more regional climate signal. We
251 focus here on two time periods (early to mid-Holocene and late Holocene), in order to test this
252 hypothesis across the Mediterranean, and to compare the results with regional climate
253 simulations for the same time periods.

254 Early to mid-Holocene (8000 to 6000 cal yrs BP)

255 Climatic patterns reconstructed from both marine and terrestrial pollen records seem to
256 corroborate the hypothesis of a north-south division in precipitation regimes during the
257 Holocene (Fig 2a). Our results confirm that northern Italy was characterized by drier conditions
258 (relative to modern) while the south-central Mediterranean experienced more annual, winter
259 and summer precipitation during the early to mid-Holocene (Fig. 2a). Only Burmarrad (Malta)
260 shows drier conditions in the early to mid-Holocene (Fig 2a), although summer precipitation
261 reconstructions are marginally higher than modern at the site. Wetter summer conditions in the
262 Aegean Sea suggest a regional, wetter, climate signal over the central and eastern
263 Mediterranean. Winter precipitation in the Aegean Sea is less spatially coherent than summer
264 signal, with dry conditions in the North Aegean Sea and or near-modern conditions in the
265 Southern Aegean Sea (Figs. 2a and 3).

266 Non-pollen proxies, including marine and terrestrial biomarkers (terrestrial n-alkanes), indicate
267 humid mid-Holocene conditions in the Aegean Sea (Triantaphyllou et al., 2014, 2016). Results
268 within the Aegean support the pollen-based reconstructions, but non-pollen proxy data are still
269 lacking at the basin scale in the Mediterranean, limiting our ability to undertake independent
270 evaluation of precipitation reconstructions.

271 Very few large-scale climate reconstruction of precipitation exist for the whole Holocene
272 (Bartlein et al., 2011; Mauri et al., 2014; Guiot and Kaniewski, 2015; Tarroso et al., 2016) and,
273 even at local scales, pollen-inferred reconstructions of seasonal precipitation are very rare (Wu
274 et al., 2007; Peyron et al., 2011, 2013; Combourieu-Nebout et al., 2013; Nourelbait et al., 2016).
275 Several studies focused on the 6000 cal years BP period; Wu et al. (2007) reconstruct regional
276 seasonal and annual precipitation and suggest that precipitation did not differ significantly from

277 modern conditions across the Mediterranean; however, scaling issues render it difficult to
278 compare their results with the reconstructions presented here. Cheddadi et al. (1997) reconstruct
279 wetter-than-modern conditions at 6000 yrs cal BP in southern Europe; however, their study uses
280 only one record from Italy and measures the moisture availability index, which is not directly
281 comparable to precipitation *sensu stricto,* since it integrates temperature and precipitation. At
282 6000 yrs cal BP, Bartlein et al. (2011) reconstruct Mediterranean precipitation at values between
283 100 and 500 mm higher than modern. Mauri et al. (2015), in an updated version of Davis et al.
284 (2003), provide a quantitative climate reconstructions comparable to the seasonal precipitation
285 reconstructions presented here. Compared to Davis et al. (2003), which focused on reconstruction
286 of temperatures, Mauri et al. (2015) reconstructed seasonal precipitation for Europe and analyse
287 their evolution throughout the Holocene. Mauri et al. (2015) results differ from the current study
288 in using MAT with plant functional type scores and in producing gridded climate maps. Mauri
289 et al. (2015) show wet summers in southern Europe (Greece and Italy) with a precipitation
290 maximum between 8000 and 6000 cal yrs BP, where precipitation was ~20 mm/month higher
291 than modern. As in our reconstruction, precipitation changes in the winter were small and not
292 significantly different from present-day conditions. Our reconstructions are in agreement with
293 Mauri et al. (2015), with similar to present day summer conditions above 45°N during the early
294 Holocene and wetter than today summer conditions over much of the south-central
295 Mediterranean south of 45°N, while winter conditions appear to be similar to modern values.
296 Mauri et al. (2015) results inferred from terrestrial pollen records and the climatic trends
297 reconstructed here from marine and terrestrial pollen records seem to corroborate the hypothesis
298 of a north-south division in precipitation regimes during the early to mid-Holocene in central
299 Mediterranean. However, more high-resolution above 45°N are still needed to validate this
300 hypothesis.

301 Late Holocene (4000 to 2000 cal yrs BP)

302 Late Holocene reconstructions of winter and summer precipitation indicate that the pattern
303 established during the early Holocene was reversed by 4000 cal yrs BP, with similar to present
304 day or lower than present day precipitation in southern Italy, Malta and Siculo-Tunisian strait
305 (Figs. 2b and 3). Annual precipitation reconstructions suggest drying relative to the early
306 Holocene, with modern conditions in northern Italy, and modern conditions or drier than
307 modern conditions in central and southern Italy during most of the late Holocene.
308 Reconstructions for the Aegean Sea still indicate higher than modern summer and annual
309 precipitation (Fig. 2b). Winter conditions reverse the early to mid-Holocene trend, with modern

310 conditions in the northern Aegean Sea and wetter than modern conditions in the southern
311 Aegean Sea (Fig. 3). Our reconstructions from all sites show a good fit with Mauri et al. (2015),
312 except for the Alboran Sea where we reconstruct relatively high annual precipitations, whereas
313 Mauri et al. (2015) reconstruct dry conditions, but here too, more sites are needed to confirm
314 or refute this pattern in Spain. Our reconstruction of summer precipitation for the eastern
315 Mediterranean is very similar to Mauri et al. (2015) where wet conditions are reported for
316 Greece and the Aegean Sea.

317
318 *An East-West precipitation pattern?*
319 A precipitation gradient, or an east-west division during the Holocene has been suggested for
320 the Mediterranean from pollen data and lakes isotopes (e.g. Dormoy et al., 2009; Roberts et al.,
321 2011; Guiot and Kaniewski, 2015). However, lake-levels and other hydrological proxies around
322 the Mediterranean Basin do not clearly support this hypothesis and rather show contrasting
323 hydrological patterns south and north of 40°N particularly during the Holocene climatic
324 optimum (Magny et al., 2013).

325 Early to mid-Holocene (8000 to 6000 cal yrs BP)

326 The pollen-inferred annual precipitation indicates unambiguously wetter than today conditions
327 south of 42°N in the western, central and eastern Mediterranean, except for Malta (Fig. 3). A
328 prominent feature of the summer precipitation signal is an east-west dipole with increasing
329 precipitation in the eastern Mediterranean (as for annual precipitation). In contrast, winter
330 conditions show less spatial coherence, although the western basin, Sicily and the Siculo-
331 Tunisian strait appear to have experienced higher precipitation than modern, while drier
332 conditions exist in the east and in north Italy (Fig. 2a).

333 Our reconstruction shows a good match to Guiot and Kaniewski (2015) who have also discussed
334 a possible east-to-west division in the Mediterranean with regard to precipitation (summer and
335 annual) during the Holocene. They report wet centennial-scale spells in the eastern
336 Mediterranean during the early Holocene (until 6000 years BP), with dry spells in the western
337 Mediterranean. Mid-Holocene reconstructions show continued wet conditions, with drying
338 through the late Holocene (Guiot and Kaniewski, 2015). This pattern indicates a see-saw effect
339 over the last 10,000 years, particularly during dry episodes in the Near and Middle East. Similar
340 to in our findings, Mauri et al. (2015) also reconstruct high annual precipitation values over
341 much of the southern Mediterranean, and a weak winter precipitation signal. Mauri et al. (2015)
342 confirm an east-west dipole for summer precipitation, with conditions drier or close to present

in south-western Europe and wetter in the central and eastern Mediterranean (Fig 2b). These studies corroborate the hypothesis of an east-to-west division in precipitation during the early to mid-Holocene in the Mediterranean as proposed by Roberts et al. (2011). Roberts et al. (2011) suggest the eastern Mediterranean (mainly Turkey and more eastern regions) experienced higher winter precipitation during the early Holocene, followed by an oscillatory decline after 6000 yrs BP. Our findings reveal wetter annual and summer conditions in the eastern Mediterranean, although the winter precipitation signal is less clear. However, the highest precipitation values reported by Roberts et al. (2011) were from sites located in western-central Turkey; these sites are absent in the current study. Climate variability in the eastern Mediterranean during the last 6000 years is also documented in a number of studies based on multiple proxies (Finné et al., 2011). Most palaeoclimate proxies indicate wet mid-Holocene conditions (Bar-Matthews et al., 2003; Stevens et al., 2006; Eastwood et al., 2007; Kuhnt et al., 2008; Verheyden et al., 2008) which agree well with our results; however most of these proxies are not seasonally resolved.

Roberts et al. (2011) and Guiot and Kaniewski (2015) suggest that changes in precipitation in the western Mediterranean were smaller in magnitude during the early Holocene, while the largest increases occurred during the mid-Holocene, around 6000-3000 cal BP, before declining to modern values. Speleothems from southern Iberia suggest a humid early Holocene (9000-7300 cal BP) in southern Iberia, with equitable rainfall throughout the year (Walczak et al., 2015) whereas our reconstructions for the Alboran Sea clearly show an amplified precipitation seasonality (with higher annual/winter and similar to modern summer rainfall) for the Alboran sites. It is likely that seasonal patterns defining the Mediterranean climate must have been even stronger in the early Holocene to support the wider development of sclerophyll forests than present in south Spain (Fletcher et al., 2013).

Late Holocene (4000 to 2000 cal yrs BP)

Annual precipitation reconstructions suggest drier or near-modern conditions in central Italy, Adriatic Sea, Siculo-Tunisian strait and Malta (Figs. 2b and 3). In contrast, the Alboran and Aegean Seas remain wetter. Winter and summer precipitation produce opposing patterns; a clear east-west division still exists for summer precipitation, with a maximum in the eastern and a minimum over the western and central Mediterranean (Fig. 2b). Winter precipitation shows the opposite trend, with a minimum in the central Mediterranean (Sicily, Siculo-Tunisian strait and Malta) and eastern Mediterranean, and a maximum in the western Mediterranean (Figs. 2b and 3). Our results are also in agreement with lakes and speleothem isotope records

over the Mediterranean for the late Holocene (Roberts et al., 2011), and the Finné et al. (2011) palaeoclimate synthesis for the eastern Mediterranean. There is a good overall correspondence between trends and patterns in our reconstruction and that of Mauri et al. (2015), except for the Alboran Sea. High-resolution speleothem data from southern Iberia show Mediterranean climate conditions in southern Iberia between 4800 and 3000 cal BP (Walczak et al., 2015) which is in agreement with our reconstruction. The Mediterranean climate conditions reconstructed here for the Alboran Sea during the late Holocene is consistent with a climate reconstruction available from the Middle Atlas (Morocco), which show a trend over the last 6000 years towards arid conditions as well as higher precipitation seasonality between 4000 and 2000 cal yrs BP (Nourelbait et al., 2016). There is also good evidence from many records to support late Holocene aridification in southern Iberia. Paleoclimatic studies document a progressive aridification trend since ~7000 cal yr BP (e.g. Carrion et al., 2010; Jimenez-Moreno et al., 2015; Ramos-Roman et al., 2016), although a reconstruction of the annual precipitation inferred from pollen data with the Probability Density Function method indicate stable and dry conditions in the south of the Iberian Peninsula between 9000 and 3000 cal BP (Tarroso et al., 2016).

The current study shows that a prominent feature of late Holocene climate is the east-west division in summer precipitation: summers were overall dry or near-modern in the central and western Mediterranean and clearly wetter in the eastern Mediterranean. In contrast, winters were drier or near-modern in the central and eastern Mediterranean (Fig. 3) while they were wetter only in the Alboran Sea.

Data-model comparison

Figure 3 shows the data-model comparisons for the early to mid-Holocene (a) and late Holocene (b) compared to present values (in anomalies). Encouragingly, there is a good overall correspondence between patterns and trends in pollen-inferred precipitation and model outputs. Caution is required when interpreting climate model results, however, as many of the changes depicted in Fig. 3 are very small and of marginal statistical significance, suggesting a high degree of uncertainty around their robustness.

For the early to mid-Holocene, both model and data indicate wet annual and summer conditions in Greece and in the eastern Mediterranean, and drier than today conditions in north Italy. There are indications of an east to west division in summer precipitation simulated by the climate

model (e.g., between the ocean to the south of Italy and over Greece/Turkey), although the changes are extremely small with a level of significance of 70%. Furthermore, in the Aegean Sea, the model shows a good match with pollen-based reconstructions, suggesting that the increased spatial resolution of the regional climate model may help to simulate the localized, "patchy", impacts of Holocene climate change, when compared to coarser global GCMs (Fig. 3). In Italy, the model shows a good match with pollen-based reconstructions with regards to the contrasting north-south precipitation regimes, but there is little agreement between model output and climate reconstruction with regard to winter and annual precipitation in southern Italy. The climate model suggests wetter winter and annual conditions in the far western Mediterranean (i.e. France, western Iberia and the NW coast of Africa) – similar to pollen-based reconstructions – and near-modern summer conditions during summers (except in France and northern Africa). A prominent feature of winter precipitation simulated by the model and partly supported by the pollen estimates is the reduced early Holocene precipitation everywhere in the Mediterranean basin except in the south east.

Model and pollen-based reconstructions for the late Holocene indicate declining winter precipitation in the eastern Mediterranean and southern Italy (Sicily and Malta) relative to the early Holocene. In contrast, late Holocene summer precipitation is higher than today in Greece and in the eastern Mediterranean and near-modern in the central and western Mediterranean, and relatively lower than today in south Spain and north Africa. The east-west division in summer precipitation is strongest during the late Holocene in the proxy data and there are suggestions that it appears to be consistently simulated in the climate model; the signal is reasonably clear in the eastern Mediterranean (Greece and Turkey) but non-significant in central and western Mediterranean (Fig. 3).

Our findings can be compared with previous data-model comparisons based on the same set of climate model experiments; although here we take our reference period as 'present-day' (1960-1990) rather than preindustrial and thus include an additional 'signal' from recent anthropogenic greenhouse gas emissions. Previous comparisons nevertheless suggested that the winter precipitation signal was strongest in the northeastern Mediterranean (near Turkey) during the early Holocene and that there was a drying trend in the Mediterranean from the early Holocene to the late Holocene, particularly in the east (Brayshaw et al., 2011a; Roberts et al., 2011). This is coupled with a gradually weakening seasonal cycle of surface air temperatures towards the present.

It is clear that most global climate models (PMIP2, PMIP3) simulate only very small changes in summer precipitation in the Mediterranean during the Holocene (Braconnot et al., 2007a,b, 2012; Mauri et al., 2014). The lack of a summer precipitation signal is consistent with the failure of the northeastern extension of the West African monsoon to reach the southeastern Mediterranean, even in the early to-mid-Holocene (Brayshaw et al., 2011a). The regional climate model simulates a small change in precipitation compared to the proxy results, and it can be robustly identified as statistically significant. This is to some extent unsurprising, insofar as the regional climate simulations presented here are themselves "driven" by data derived from a coarse global model (which, like its PMIP2/3 peers, does not simulate an extension of the African monsoon into the Mediterranean during this time period). Therefore, questions remain about summer precipitation in the eastern Mediterranean during the Holocene. The underlying climate dynamics therefore need to be better understood in order to confidently reconcile proxy data (which suggest increased summer precipitation during the early Holocene in the Eastern Mediterranean) with climate model results (Mauri et al., 2014). Based on the high-resolution coupled climate model EC-Earth, Bosmans et al. (2015) show how the seasonality of Mediterranean precipitation should vary from minimum to maximum precession, indicating a reduction in precipitation seasonality, due to changes in storm tracks and local cyclogenesis (i.e. no direct monsoon required). Such high-resolution climate modeling studies (both global and regional) may prove a key ingredient in simulating the relevant atmospheric processes (both local and remote) and providing fine-grain spatial detail necessary to compare results to palaeo-proxy observations.

Another explanation proposed by Mauri et al. (2014) is linked to the changes in atmospheric circulation. Our reconstructed climate characterized by dry winters and wet summers shows a spatial pattern that is somewhat consistent with modern day variability in atmospheric circulation rather than simple direct radiative forcing by insolation. In particular, the gross NW-SE dipole of reconstructed winter precipitation anomalies is perhaps similar to that associated with a modern-day positive AO/NAO. The west coast of Spain is, however, also wetter in our early Holocene simulations which would seem to somewhat confound this simple picture of a shift to an NAO+ like state compared to present. In summer, an anti-cyclonic blocking close to Scandinavia may have caused a more meridional circulation, which brought dry conditions to northern Europe, but relatively cooler and somewhat wetter conditions to many parts of southern Europe. It is of note that some climate models which have been used for studying palaeoclimate have difficulty reproducing this aspect of modern climate (Mauri et al., 2014).

Future work based on transient Holocene model simulations are important, nevertheless, transient-model simulations have also shown mid-Holocene data-model discrepancies (Fischer and Jungclaus, 2011; Renssen et al., 2012). It is, however, suggested that further work is required to fully understand changes in winter and summer circulation patterns over the Mediterranean (Bosmans et al., 2015).

Data limitations

Classic ecological works for the Mediterranean (e.g. Ozenda 1975) highlight how precipitation limits vegetation type in plains and lowland areas, but temperature gradients take primary importance in mountain systems. Also, temperature and precipitation changes are not independent, but interact through bioclimatic moisture availability and growing season length (Prentice et al., 1996). This may be one reason why certain sites may diverge from model outputs; the Alboran sites, for example, integrate pollen from the coastal plains through to mountain (+1500m) elevations. At high elevations within the source area, temperature effects become be more important than precipitation in determining the forest cover type. Therefore, it is not possible to fully isolate precipitation signals from temperature changes. Particularly for the semiarid areas of the Mediterranean, the reconstruction approach probably cannot distinguish between a reduction in precipitation and an increase in temperature and PET, or vice versa.

Along similar lines, while the concept of reconstructing winter and summer precipitation separately is very attractive, it may be highlighting commenting on some limitations. Although different levels of the severity or length of summer drought are an important ecological limitation for vegetation, reconstructing absolute summer precipitation can be difficult because the severity/length of bioclimatic drought is determined by both temperature and precipitation. We are dealing with a season that has, by definition, small amounts of precipitation that drop below the requirements for vegetation growth. Elevation is also of concern, as lowland systems tend to be recharged by winter rainfall, but high mountain systems may receive a significant part of precipitation as snowfall, which is not directly available to plant life. This may be important in the long run for improving the interpretation of long-term Holocene changes and contrasts between different proxies, such as lake-levels and speleothems. All of these points may seem very picky on the ecology side, but they may have a real influence leading to problems and mismatches between different proxies (e.g. Davis et al., 2003; Mauri et al., 2015).

505 Another important point is the question of human impact on the Mediterranean vegetation
506 during the Holocene. Since human activity has influenced natural vegetation, distinguishing
507 between vegetation change induced by humans and climatic change in the Mediterranean is a
508 challenge requiring independent proxies and approaches. Therefore links and processes behind
509 societal change and climate change in the Mediterranean region are increasingly being
510 investigated (e.g. Holmgren et al., 2016; Gogou et al, 2016; Sadori et al., 2016a). Here, the
511 behavior of the reconstructed climatic variables between 4000 and 2000 cal yrs BP is likely
512 to be influenced by non-natural ecosystem changes due to human activities such as the forest
513 degradation that began in lowlands, progressing to mountainous areas (Carrión et al., 2010).
514 These human impacts add confounding effects for fossil pollen records and may lead to slightly
515 biased temperature reconstructions during the late Holocene, likely biased towards warmer
516 temperatures and lower precipitation. However, if human activities become more marked at
517 3000 cal yrs BP, they increase significantly over the last millennia (Sadori et al., 2016) which
518 is not within the time scale studied here. Moreover there is strong agreement between summer
519 precipitation and independently reconstructed lake-level curves (Magny et al., 2013). For the
520 marine pollen cores, human influence is much more difficult to interpret given that the source
521 area is so large, and that, in general, anthropic taxa are not found in marine pollen assemblages.
522

523 **Conclusions**

524 The Mediterranean is particularly sensitive to climate change but the extent of future change
525 relative to changes during the Holocene remains uncertain. Here, we present a reconstruction
526 of Holocene precipitation in the Mediterranean using an approach based on both terrestrial and
527 marine pollen records, along with a model-data comparison based on a high resolution regional
528 model. We investigate climatic trends across the Mediterranean during the Holocene to test the
529 hypothesis of an alternating north-south precipitation regime, and/or an east-west precipitation
530 dipole. We give particular emphasis to the reconstruction of seasonal precipitation considering
531 the important role it plays in this system.

532 Climatic trends reconstructed in this study seem to corroborate the north-south division of
533 precipitation regimes during the Holocene, with wet conditions in the south-central and eastern
534 Mediterranean, and dry conditions above 45°N during the early Holocene, while the opposite
535 pattern dominates during the late Holocene. This study also shows that a prominent feature of
536 Holocene climate in the Mediterranean is the east-to-west division in precipitation, strongly
537 linked to the seasonal parameter reconstructed. During the early Holocene, we observe an east-

538 to-west division with high summer precipitation in Greece and the eastern Mediterranean and
539 a minimum over the Italy and the western Mediterranean. There was a drying trend in the
540 Mediterranean from the early Holocene to the late Holocene, particularly in central and eastern
541 regions but summers in the east remained wetter than today. In contrast, the signal for winter
542 precipitation is less spatially consistent during the early Holocene, but it clearly shows similar
543 to present day or drier conditions everywhere in the Mediterranean except in the western basin
544 during the late Holocene.

545 The regional climate model outputs show a remarkable qualitative agreement with our pollen-
546 based reconstructions, although it must be emphasised that the changes simulated are typically
547 very small or of questionable statistical significance. Nevertheless, there are indications that the
548 east to west division in summer precipitation reconstructed from the pollen records do appear
549 to be simulated by the climate model. The model results also suggest that parts of the eastern
550 Mediterranean experienced similar to present day or drier conditions in winter during the early
551 and late Holocene and wetter conditions in annual and summer during the early and late
552 Holocene (both consistent with the paleo-records).

553 Although this study has used regional climate model data, it must always be recalled that the
554 regional model's high-resolution output is strongly constrained by a coarser-resolution global
555 climate model, and the ability of global models to correctly reproduce large-scale patterns of
556 change in the Mediterranean over the Holocene remains unclear (e.g. Mauri et al 2015). The
557 generally positive comparison between model and data presented here may therefore simply be
558 fortuitous and not necessarily replicated if the output from other global climate model
559 simulations was downscaled in a similar way. However, it is noted that the use of higher-
560 resolution regional climate models can offer significant advantages for data-model comparison
561 insofar as they assist in resolving the inherently "patchy" nature of climate signals and palaeo-
562 records. Notwithstanding the difficulties of correctly modeling large-scale climate change over
563 the Holocene (with GCMs), we believe that regional downscaling may still be valuable in
564 facilitating model-data comparison in regions/locations known to be strongly influenced by
565 local effects (e.g., complex topography).

566

Acknowledgements

This study is a part of the LAMA ANR Project (MSHE Ledoux, USR 3124, CNRS) financially supported by the French CNRS (National Centre for Scientific Research). Simon Goring is currently supported by NSF Macrosystems grant 144-PRJ45LP. This is an ISEM contribution n°XXXX.

Figure captions

Figure 1: Locations of terrestrial and marine pollen records along a longitudinal gradient from west to east and along a latitudinal gradient from northern Italy to Malta. Ombrothermic diagrams are shown for each site, calculated with the NewLoclim software program and database, which provides estimates of average climatic conditions at locations for which no observations are available (ex.: marine pollen cores).

Figure 2: Pollen-inferred climate estimates as performed with the Modern Analogues Technique (MAT): annual precipitation, winter precipitation (winter = sum of December, January and February precipitation) and summer precipitation (summer = sum of June, July and August precipitation). Changes in climate are expressed as differences with respect to the modern values (anomalies, mm/day). The modern values are derived from the ombrothermic diagrams (cf Fig. 1). Two key intervals of the Holocene corresponding to the two time slice experiments (Fig. 3) have been chosen: 8000–6000 cal yrs BP (a) and 4000–2000 (b) cal yrs BP. The climate values available during these periods have been averaged (stars).

Figure 3: Data-model comparison for mid and late Holocene precipitation, expressed in anomaly compared to present-day (mm/day). Simulations are based on a regional model (Brayshaw et al., 2010): standard model HadAM3 coupled to HadSM3 (dynamical model) and HadRM3 (high-resolution regional model. The hatched areas indicate areas where the changes are not significant (70% rank-significance test). Pollen-inferred climate estimates (stars) are the same as in Fig. 2: annual precipitation, winter precipitation (winter = sum of December, January and February precipitation) and summer precipitation (summer = sum of June, July and August precipitation).

Figure 4: Model simulation showing Present day minus Preindustrial precipitation anomalies (hatching at 70%/statistical significance over the insignificant regions)

Table 1: Metadata for the terrestrial and marine pollen records evaluated.

References

Alpert, P., Baldi, M., Ilani, R., Krichak, S., Price, C., Rodó, X., Saaroni, H., Ziv, B., Kishcha, P., Barkan, J., Mariotti, A. and Xoplaki, E.: Relations between climate variability in the Mediterranean region and the Tropics: ENSO, South Asian and African monsoons, hurricanes and Saharan dust In: Lionello P, Malanotte-Rizzoli P, Boscolo R (eds) Mediterranean Climate Variability, Amsterdam, Elsevier 149-177, 2006.

Bar-Matthews, M., Ayalon, A., Gilmour, M., Matthews, A. and Hawkesworth, C.J.: Sea-land oxygen isotopic relationships from planktonic foraminifera and speleothems in the Eastern Mediterranean region and their implication for paleorainfall during interglacial intervals, Geochimica et Cosmochimica Acta 67, 3181-3199, 2003.

Bar-Matthews, M. and Ayalon, A.: Mid-Holocene climate variations revealed by high-resolution speleothem records from Soreq Cave, Israel and their correlations with cultural changes, Holocene, 21, 163–172, 2011.

Bartlein, P.J., Harrison, S.P., Brewer, S., Connor, S., Davis, B.A.S., Gajewski, K., Guiot, J., Harrison-Prentice, T.I., Henderson, A., Peyron, O., Prentice, I.C., Scholze, M., Seppä, H., Shuman, B., Sugita, S., Thompson, R.S., Viau, A.E, Williams, J., and Wu H.: Pollen-based continental climate reconstructions at 6 and 21 ka: a global synthesis, Climate Dynamics 37, 775-802, 2011.

Bosmans, J.H.C., Drijfhout, S.S., Tuenter, E., Hilgen, F.J., Lourens, L.J. and Rohling, E.J.: Precession and obliquity forcing of the freshwater budget over the Mediterranean, Quaternary Science Reviews, 123, 16-30, 2015.

Braconnot, P., Otto-Bliesner, B., Harrison, S., Joussaume, S., Peterchmitt, J.-Y., Abe-Ouchi, A., Crucifix, M., Driesschaert, E., Fichefet, Th., Hewitt, C. D., Kageyama, M., Kitoh, A., Laîné, A., Loutre, M.-F., Marti, O., Merkel, U., Ramstein, G., Valdes, P., Weber, S. L., Yu, Y., and Zhao, Y.: Results of PMIP2 coupled simulations of the Mid-Holocene and Last Glacial Maximum –Part 1: experiments and large-scale features, Clim. Past, 3, 261–277, 2007a.

Braconnot, P., Otto-Bliesner, B., Harrison, S., Joussaume, S., Peterchmitt, J.-Y., Abe-Ouchi, A., Crucifix, M., Driesschaert, E., Fichefet, Th., Hewitt, C. D., Kageyama, M., Kitoh, A., Loutre, M.-F., Marti, O., Merkel, U., Ramstein, G., Valdes, P., Weber, L., Yu, Y., and Zhao, Y.: Results of PMIP2 coupled simula-tions of the Mid-Holocene and Last Glacial Maximum – Part 2: feedbacks with emphasis on the location of the ITCZ and mid- and high latitudes heat budget, Clim. Past, 3, 279–296, 2007b.

632   Braconnot, P., Harrison, S., Kageyama, M., Bartlein, J., Masson, V., Abe-Ouchi, A., Otto-

633   Bliesner, B., and Zhao, Y.: Evaluation of climate models using palaeoclimatic data, Nat. Clim.

634   Change, 2, 417-424, 2012.

635   Brayshaw, D.J., Hoskins, B. and Black, E.: Some physical drivers of changes in the winter

636   storm tracks over the North Atlantic and Mediterranean during the Holocene. Philosophical

637   Transactions of the Royal Society A: Mathematical, Physical and Engineering Sciences, 368,

638   5185-5223, 2010.

639   Brayshaw, D.J., Rambeau, C.M.C., and Smith, S.J.: Changes in the Mediterranean climate

640   during the Holocene: insights from global and regional climate modelling, Holocene 21, 15-31,

641   2011a.

642   Brayshaw, D.J., Black, E., Hoskins, B. and Slingo, J.: Past climates of the Middle East, In:

643   Mithen, S. and Black, E. (eds.) Water, Life and Civilisation: Climate, Environment and Society

644   in the Jordan Valley. International Hydrology Series. Cambridge University Press, Cambridge,

645   pp. 25-50, 2011b

646   Carrión, J.S., Fernández, S., Jiménez-Moreno, G., Fauquette, S., Gil-Romera, G., González-

647   Sampériz, P. and Finlayson, C.: The historical origins of aridity and vegetation degradation in

648   southeastern Spain, Journal of Arid Environments, 74, 731-736, 2010.

649   Cheddadi, R., Yu, G., Guiot, J., Harrison, S.P., and Prentice, I.C.: The climate of Europe 6000

650   years ago, Climate Dynamics 13, 1-9, 1997.

651   Colmenero-Hidalgo, E., Flores, J.-A., and Sierro, F.J. Biometry of Emiliania huxleyi and its

652   biostratigraphic significance in the eastern north Atlantic Ocean and Western Mediterranean

653   Sea in the last 20,000 years, Marine Micropaleontology, 46, 247-263, 2002.

654   Colombaroli, D., Vannière, B., Chapron, E., Magny, M., and Tinner, W. Fire–vegetation

655   interactions during the Mesolithic–Neolithic transition at Lago dell'Accesa, Tuscany, Italy, The

656   Holocene, 18, 679–692, 2008.

657   Combourieu-Nebout, N., Paterne, M., Turon, J.-L., and Siani, G.: A high-resolution record of

658   the Last Deglaciation in the Central Mediterranean Sea: palaeovegetation and

659   palaeohydrological evolution, Quaternary Sci. Rev., 17, 303–332, 1998.

660   Combourieu-Nebout, N., Londeix, L., Baudin, F., and Turon, J.L.: Quaternary marine and

661   continental palaeoenvironments in the Western Mediterranean Sea (Leg 161, Site 976, Alboran

662 Sea): Palynological evidences, Proceeding of the Ocean Drilling Project, scientific results, 161,
663 457-468, 1999.

664 Combourieu-Nebout, N., Turon, J.L., Zahn, R., Capotondi, L, Londeix, L., and Pahnke, K.:
665 Enhanced aridity and atmospheric high pressure stability over the western Mediterranean
666 during North Atlantic cold events of the past 50 000 years, Geology, 30, 863-866, 2002.

667 Combourieu-Nebout, N., Peyron, O., Dormoy, I., Desprat, S., Beaudouin, C., Kotthoff, U., and
668 Marret, F.: Rapid climatic variability in the west Mediterranean during the last 25 000 years
669 from high resolution pollen data, Clim. Past, 5, 503-521, 2009.

670 Combourieu-Nebout, N., Peyron, O., Bout-Roumazeilles, V., Goring, S., Dormoy, I., Joannin,
671 S., Sadori, L., Siani, G., and Magny, M.: Holocene vegetation and climate changes in
672 central Mediterranean inferred from a high-resolution marine pollen record (Adriatic Sea),
673 Clim. Past 9, 2023-2042, 2013.

674 Davis, B. A. S., Brewer, S., Stevenson, A. C., and Guiot, J.: The temperature of Europe during
675 the Holocene reconstructed from pollen data, Quaternary Sci. Rev., 22, 1701–1716, 2003.

676 Davis, B. A. S. and Brewer, S.: Orbital forcing and role of the latitudinal insolation/ temperature
677 gradient, Clim. Dynam., 32, 143-165, 2009.

678 De Santis V. and Caldara M. The 5.5–4.5 kyr climatic transition as recorded by the
679 sedimentation pattern of coastal deposits of the Apulia region, southern Italy, Holocene, 2015

680 Desprat, S., Combourieu-Nebout, N., Essallami, L., Sicre, M. A., Dormoy, I., Peyron, O.,
681 Siani, G., Bout Roumazeilles, V., and Turon, J. L.: Deglacial and Holocene vegetation
682 and climatic changes in the southern Central Mediterranean from a direct land-sea
683 correlation, Clim. Past, 9, 767–787, 2013.

684 Djamali, M., Gambin, B., Marriner, N., Andrieu-Ponel, V., Gambin, T., Gandouin, E., Médail,
685 F., Pavon, D., Ponel, P., and Morhange, C.: Vegetation dynamics during the early to mid-
686 Holocene transition in NW Malta, human impact versus climatic forcing, Vegetation History
687 and Archaeobotany 22, 367-380, 2013.

688 Dormoy, I., Peyron, O., Combourieu Nebout, N., Goring, S., Kotthoff, U., Magny, M, and
689 Pross, J.: Terrestrial climate variability and seasonality changes in the Mediterranean region
690 between 15,000 and 4,000 years B.P. deduced from marine pollen records, Clim. Past, 5, 615-
691 632, 2009.

692 Drescher-Schneider, R., de Beaulieu, J.L., Magny, M., Walter-Simonnet, A.V., Bossuet, G.,
693 Millet, L. Brugiapaglia, E., and Drescher A.: Vegetation history, climate and human impact
694 over the last 15 000 years at Lago dell'Accesa, Veg. Hist. Archaeobot., 16, 279–299, 2007.

695 Eastwood, WJ., Leng, M., Roberts, N. and Davis B.: Holocene climate change in the eastern
696 Mediterranean region: a comparison of stable isotope and pollen data from Lake Gölhisar,
697 southwest Turkey, J. Quaternary Science 22, 327–341, 2007.

698 Finné, M., Holmgren, K., Sundqvist, H.S., Weiberg, E., and Lindblom, M.: Climate in the
699 eastern Mediterranean, and adjacent regions, during the past 6000 years, J. Archaeol. Sci., 38,
700 3153-3173, 2011.

701 Fischer N., and Jungclaus, J. H.: Evolution of the seasonal temperature cycle in a transient
702 Holocene simulation: orbital forcing and sea-ice, Clim. Past, 7, 1139-1148, 2011.

703 Fletcher, W.J., and Sánchez Goñi, M.F.: Orbital- and sub-orbital-scale climate impacts on
704 vegetation of the western Mediterranean basin over the last 48,000 yr, Quat. Res. 70, 451-464,
705 2008.

706 Fletcher, W.J., Sanchez Goñi, M.F., Peyron, O., and Dormoy, I.: Abrupt climate changes of the
707 last deglaciation detected in a western Mediterranean forest record, Clim. Past 6, 245-264, 2010.

708 Fletcher, W.J., Debret, M., and Sanchez Goñi, M.F.: Mid-Holocene emergence of a low-
709 frequency millennial oscillation in western Mediterranean climate: Implications for past
710 dynamics of the North Atlantic atmospheric westerlies, The Holocene, 23, 153-166, 2013.

711 Gambin B., Andrieu-Ponel V., Médail F., Marriner N., Peyron O., Montade V., Gambin T.,
712 Morhange C., Belkacem D., and Djamali M.: 7300 years of vegetation history and quantitative
713 climate reconstruction for NW Malta: a Holocene perspective, Clim. Past 12, 273-297, 2016

714 Geraga, M., Ioakim, C., Lykousis, V., Tsaila-Monopolis, S., and Mylona, G.: The high-
715 resolution palaeoclimatic and palaeoceanographic history of the last 24,000 years in the central
716 Aegean Sea, Greece, Palaeogeogr. Palaeocl., 287, 101–115, 2010.

717 Giorgi, F. and Lionello, P.: Climate change projections for the Mediterranean region, Global
718 Planet. Change, 63, 90–104, 2008.

719 Gogou, A., Bouloubassi, I., Lykousis, V., Arnaboldi, M., Gaitani, P., and Meyers, P.A.: Organic
720 geochemical evidence of abrupt late glacial- Holocene climate changes in the North Aegean
721 Sea, Palaeogeogr. Palaeocl., 256, 1 – 20, 2007.

722 Gogou, A., Triantaphyllou, M., Xoplaki, E., Izdebski, A., Parinos, C., Dimiza, M., Bouloubassi,
723 I., Luterbacher, J., Kouli, K., Martrat, B., Toreti, A., Fleitmann, D., Rousakis, G., Kaberi, H.,
724 Athanasiou, M., and Lykousis, V.: Climate variability and socio-environmental changes in the
725 northern Aegean (NE Mediterranean) during the last 1500 years, Quaternary Science Reviews,
726 136, 209-228, 2016.

727 Guiot J.: Methodology of the last climatic cycle reconstruction in France from pollen data,
728 Palaeogeography, Palaeoclimatology, Palaeoecology, 80, 49–69, 1990.

729 Guiot, J. and Kaniewski, D.: The Mediterranean Basin and Southern Europe in a warmer world:
730 what can we learn from the past? Front. Earth Sci., 18, 2015.

731 Hargreaves, J.C., Annan, J.D., Ohgaito, R., Paul, A., and Abe-Ouchi, A.: Skill and reliability
732 of climate model ensembles at the Last Glacial Maximum and mid-Holocene, Clim. Past, 9,
733 811-823, 2013.

734 Heiri, O., Brooks, S.J., Renssen, H., and 26 authors: Validation of climate model-inferred
735 regional temperature change for late-glacial Europe, Nature Communications 5, 4914, 2014.

736 Heusser, L.E., and Balsam W.L.: Pollen distribution in the N.E. Pacific ocean, Quaternary
737 Research, 7, 45-62, 1977.

738 Hewitt, C.D., Senior, C.A., and Mitchell, J.F.B. :The impact of dynamic sea-ice on the
739 climatology and sensitivity of a GCM: A study of past, present and future climates, Climate
740 Dynamics 17: 655–668, 2001.

741 Holmgren, K., Gogou, A., Izdebski, A., Luterbacher, J., Sicre, M.A., and Xoplaki, A.:
742 Mediterranean Holocene Climate, Environment and Human Societies, Quaternary Science
743 Reviews, 136, 1-4, 2016.

744 Ioakim, Chr., Triantaphyllou, M., Tsaila-Monopolis, S., and Lykousis, V.: New
745 micropalaeontological records of Eastern Mediterranean marine sequences recovered offshore
746 of Crete, during HERMES cruise and their palaeoclimatic paleoceanographic significance. Acta
747 Naturalia de "L'Ateneo Parmense", 45(1/4): p. 152. In: Earth System Evolution and the
748 Mediterranean Area from 23 Ma to the Present", 2009.

749 Jimenez-Moreno, G., Rodriguez-Ramirez, A., Perez-Asensio, J.N., Carrion, J.S., Lopez-Saez,
750 J.A, Villarías-Robles J., Celestino-Perez, S., Cerrillo-Cuenca, E., Leon, A., and Contreras, C.:
751 Impact of late-Holocene aridification trend, climate variability and geodynamic control on the
752 environment from a coastal area in SW Spain, Holocene, 1-11, 2015

753 Joannin, S., Vannière, B., Galop, D., Peyron, O., Haas, J.N., Gilli, A., Chapron, E., Wirth, S.,
754 Anselmetti, F., Desmet, M., and Magny, M.: Climate and vegetation changes during the
755 Lateglacial and Early-Mid Holocene at Lake Ledro (southern Alps, Italy), Clim. Past 9, 913-
756 933, 2013.

757 Joannin, S., Brugiapaglia, E., de Beaulieu, J.L, Bernardo, L., Magny, M., Peyron, O., Goring,
758 S., and Vannière, B.: Pollen-based reconstruction of Holocene vegetation and climate in
759 southern Italy: the case of Lago Trifoglietti., Clim. Past, 8, 1973-1996, 2012.

760 Kotthoff, U., Pross, J., Müller, U.C., Peyron, O., Schmiedl, G., and Schulz, H. Climate
761 dynamics in the borderlands of the Aegean Sea during formation of Sapropel S1 deduced from
762 a marine pollen record, Quaternary Sci. Rev., 27, 832–845, 2008.

763 Kotthoff, U., Koutsodendris, A., Pross, J., Schmiedl, G., Bornemann, A., Kaul, C., Marino, G.,
764 Peyron, O., and Schiebel, R. Impact of late glacial cold events on the Northern Aegean region
765 reconstructed from marine and terrestrial proxy data, J. Quat. Sci., 26, 86-96, 2011.

766 Kouli, K., Gogou, A., Bouloubassi, I., Triantaphyllou, M.V., Ioakim, Chr, Katsouras, G.,
767 Roussakis, G., and Lykousis, V.: Late postglacial paleoenvironmental change in the
768 northeastern Mediterranean region: Combined palynological and molecular biomarker
769 evidence, Quatern. Int., 261, 118-127, 2012.

770 Kuhnt, T., Schmiedl, G., Ehrmann, W., Hamann, Y., and Andersen, N.: Stable isotopic
771 composition of Holocene benthic foraminifers from the eastern Mediterranean Sea: past
772 changes in productivity and deep water oxygenation, Palaeogeography, Palaeoclimatology,
773 Palaeoecology 268, 106-115, 2008.

774 Lionello, P, Malanotte-Rizzoli, P, Boscolo, R, Alpert, P, Artale, V, Li, L., et al.: The
775 Mediterranean climate: An overview of the main characteristics and issues. In: Lionello P,
776 Malanotte-Rizzoli P and Boscolo R (eds) Mediterranean Climate Variability. Developments in
777 Earth & Environmental Sciences 4, Elsevier, 1–26, 2006.

778 Lionello, P. (Ed.): The climate of the Mediterranean region: From the past to the future,
779 Elsevier, ISBN: 9780124160422, 2012.

780 Luterbacher, J., García-Herrera, R., Akcer-On, S., Allan R., Alvarez-Castro M.C, and 41
781 authors: A review of 2000 years of paleoclimatic evidence in the Mediterranean. In: Lionello,
782 P. (Ed.), The Climate of the Mediterranean region: From the past to the future, Elsevier,
783 Amsterdam, The Netherlands, 2012.

784   Magny, M., de Beaulieu, J.L., Drescher-Schneider, R., Vannière, B., Walter-Simonnet, A.V.,
785   Miras, Y., Millet, L., Bossuet, G., Peyron, O., Brugiapaglia, E., and Leroux, A.: Holocene
786   climate changes in the central Mediterranean as recorded by lake-level fluctuations at Lake
787   Accesa (Tuscany, Italy), Quaternary Sci. Rev. 26, 1736–1758, 2007.

788   Magny, M., Vannière, B., Zanchetta, G., Fouache, E., Touchais, G., Petrika, L., Coussot, C.,
789   Walter-Simonnet, A.V., and Arnaud, F.: Possible complexity of the climatic event around 4300-
790   3800 cal BP in the central and western Mediterranean, Holocene, 19, 823-833, 2009.

791   Magny, M., Vannière, B., Calo, C., Millet, L., Leroux, A., Peyron, O., Zanchetta, G., La Mantia,
792   T. and Tinner, W.: Holocene hydrological changes in south-western Mediterranean as recorded
793   by lake-level fluctuations at Lago Preola, a coastal lake in southern Sicily, Italy, Quaternary
794   Sci. Rev., 30, 2459-2475, 2011.

795   Magny, M., Joannin, S., Galop, D., Vannière, B., Haas, J.N, Bassetti, M., Bellintani, P.,
796   Scandolari, R., and Desmet, M.: Holocene palaeohydrological changes in the northern
797   Mediterranean borderlands as reflected by the lake-level record of Lake Ledro, northeastern
798   Italy, Quaternary Res., 77, 382-396, 2012a.

799   Magny, M., Peyron, O., Sadori, L., Ortu, E., Zanchetta, G., Vannière, B., and Tinner, W.:
800   Contrasting patterns of precipitation seasonality during the Holocene in the south- and north-
801   central Mediterranean, J. Quaternary Sci., 27, 290–296, 2012b.

802   Magny, M. and 29 authors: North-south palaeohydrological contrasts in the central
803   Mediterranean during the Holocene: tentative synthesis and working hypotheses, Clim. Past 9,
804   2043-2071, 2013.

805   Mauri, A., Davis, B., Collins, P.M. and Kaplan, J.: The climate of Europe during the Holocene:
806   A gridded pollen-based reconstruction and its multi-proxy evaluation, Quat. Sc. Rev. 112, 109-
807   127, 2014.

808   Mauri, A., Davis, B., Collins, P.M. and Kaplan, J.: The influence of atmospheric circulation on
809   the mid-Holocene climate of Europe: A data–model comparison, Clim. Past 10, 1925-1938,
810   2015.

811   Morrill, C., Anderson, D.M, Bauer, B.A, Buckner, R.E., Gille, P., Gross, W.S., Hartman, M.,
812   and Shah, A.: Proxy benchmarks for intercomparison of 8.2 ka simulations, Clim. Past 9, 423-
813   432, 2013.

814 Naughton, F., Sanchez Goñi, M.F., Desprat, S., Turon, J.L., Duprat, J., Malaizé, B., Joli, C.,

815 Cortijo, E., Drago, T., and Freitas, M.C.: Present-day and past (last 25 000 years) marine pollen

816 signal off western Iberia, Marine Micropaleontology 62, 91-114, 2007.

817 Nourelbait, M., Rhoujjati, A., Benkaddour, A., Carré, M., Eynaud, F., Martinez, P. and

818 Cheddadi, R.: Climate change and ecosystems dynamics over the last 6000 years in the Middle

819 Atlas, Morocco, Clim. Past 12, 1029-1042, 2016.

820 Peyron, O., Goring, S., Dormoy, I., Kotthoff, U., Pross, J., de Bealieu, J.L., Drescher-

821 Schneider, R., and Magny, M.: Holocene seasonality changes in the central Mediterranean

822 region reconstructed from the pollen sequences of Lake Accesa (Italy) and Tenaghi Philippon

823 (Greece), Holocene, 21, 131-146, 2011.

824 Peyron, O., Magny, M., Goring, S., Joannin, S., de Beaulieu, J.-L., Brugiapaglia, E., Sadori, L.,

825 Garfi, G., Kouli, K., Ioakim, C., and Combourieu-Nebout, N. Contrasting patterns of climatic

826 changes during the Holocene in the central Mediterranean (Italy) reconstructed from pollen

827 data, Clim. Past 9, 1233-2013, 2013.

828 Pope, V.D., Gallani, M.L., Rowntree, R.R. and Stratton, R.A.: The impact of new physical

829 parameterizations in the Hadley Centre climate model: HadAM3, Climate Dynamics, 16, 123-

830 146, 2000.

831 Pross, J., Kotthoff, U., Müller, U.C., Peyron, O., Dormoy, I., Schmiedl, G., Kalaitzidis, S., and

832 Smith, A.M.: Massive perturbation in terrestrial ecosystems of the Eastern Mediterranean

833 region associated with the 8.2 kyr climatic event, Geology, 37, 887-890, 2009.

834 Pross, J., Koutsodendris, A., Christanis, K., Fischer, T., Fletcher, W.J., Hardiman, M.,

835 Kalaitzidis, S., Knipping, M., Kotthoff, U., Milner, A.M., Müller, U.C., Schmiedl, G., Siavalas,

836 G., Tzedakis, P.C., and Wulf, S.: The 1.35-Ma-long terrestrial climate archive of Tenaghi

837 Philippon, northeastern Greece: Evolution, exploration and perspectives for future research,

838 Newsletters on Stratigraphy, 48, 253-276, 2015.

839 Ramos-Román, M.J., Jiménez-Moreno, G., Anderson, R.S., García-Alix, A., Toney, J.L.,

840 Jiménez-Espejo, F.J. and Carrión, J.S.: Centennial-scale vegetation and North Atlantic

841 Oscillation changes during the Late Holocene in the southern Iberia, Quaternary Science

842 Reviews, 143, 84-98, 2016.

843 Renssen, H., Seppa, H., Crosta, X., Goosse, H., and Roche, D.M.: Global characterization of

844 the Holocene Thermal Maximum, Quat. Sci. Rev., 48, 7-19, 2012.

845 Roberts, N., Brayshaw, D., Kuzucuoğlu, C., Perez, R., and Sadori, L.: The mid-Holocene
846 climatic transition in the Mediterranean: Causes and consequences, Holocene, 21, 3-13, 2011.

847 Roberts, N., Moreno, A., Valero-Garces, B. L., Corella, J. P., Jones, M., Allcock, S., et al.
848 Palaeolimnological evidence for an east-west climate see-saw in the mediterranean since AD
849 900, Glob. Planet. Change, 84-85, 23-34, 2012.

850 Rohling, E.J., Cane, T.R., Cooke, S., Sprovieri, M., Bouloubassi, I., Emeis, K.C. et al: African
851 monsoon variability during the previous interglacial maximum, Earth Planet. Sc. Lett., 202, 61-
852 75, 2002.

853 Sadori, L. and Narcisi, B.: The postglacial record of environmental history from Lago di
854 Pergusa, Sicily, Holocene, 11, 655-671, 2001.

855 Sadori, L. and Giardini, M.: Charcoal analysis, a method to study vegetation and climate of the
856 Holocene: The case of Lago di Pergusa, Sicily (Italy), Geobios-Lyon, 40, 173-180, 2007.

857 Sadori, L., Zanchetta, G., and Giardini, M.: Last Glacial to Holocene palaeoenvironmental
858 evolution at Lago di Pergusa (Sicily, Southern Italy) as inferred by pollen, microcharcoal, and
859 stable isotopes, Quatern. Int., 181, 4-14, 2008.

860 Sadori, L., Jahns, S., and Peyron, O.: Mid-Holocene vegetation history of the central
861 Mediterranean, Holocene, 21, 117-129, 2011.

862 Sadori, L., Ortu, E., Peyron, O., Zanchetta, G., Vannière, B, Desmet, M., and Magny, M.: The
863 last 7 millennia of vegetation and climate changes at Lago di Pergusa (central Sicily, Italy),
864 Clim. Past, 9, 1969-1984, 2013.

865 Sadori, L., Giraudi, C. Masi, A., Magny, M., Ortu, E., Zanchetta, G., and Izdebski, A. Climate,
866 environment and society in southern Italy during the last 2000 years. A review of the
867 environmental, historical and archaeological evidence, Quaternary Science Reviews, 136, 173-
868 188, 2016a.

869 Sadori, L., Koutsodendris, A., Masi, A., Bertini, A., Combourieu-Nebout, N., Francke, A.,
870 Kouli, K., Joannin, S., Mercuri, A.M, Panagiotopoulos, K., Peyron, O., Torri, P., Wagner, B.,
871 Zanchetta, G., and Donders, T.H.: Pollen-based paleoenvironmental and paleoclimatic change
872 at Lake Ohrid (SE Europe) during the past 500 ka, Biogeosciences, 12, 15461-15493, 2016b.

873 Schemmel, F., Niedermeyer, E.M., Schwab-Lavrič, V., Gleixner, G., Pross, J., and Mulch, A.:
874 Plant-wax dD values record changing Eastern Mediterranean atmospheric circulation patterns
875 during the 8.2 ka BP climatic event, Quaternary Science Reviews, 133, 96-107, 2016.

876 Stevens, L.R., Ito, E., Schwalb, A., and Wright, H.E.: Timing of atmospheric precipitation in
877 the Zagros Mountains inferred from a multi-proxy record from Lake Mirabad, Iran, Quat. Res.
878 66, 494-500, 2006.

879 Tarroso, P., Carrión, J., Dorado-Valiño, M., Queiroz, P., Santos, L., Valdeolmillos-Rodríguez,
880 A., Célio Alves, P., Brito, J. C., and Cheddadi, R.: Spatial climate dynamics in the Iberian
881 Peninsula since 15 000 yr BP, Clim. Past, 12, 1137-1149, 2016.

882 Triantaphyllou, V., Antonarakou, A., Kouli, K., Dimiza, M., Kontakiotis, G., Papanikolaou,
883 M.D. et al.: Late Glacial–Holocene ecostratigraphy of the south-eastern Aegean Sea, based on
884 plankton and pollen assemblages, Geo-Mar. Lett., 29, 249-267, 2009a.

885 Triantaphyllou, M.V., Ziveri, P., Gogou, A., Marino, G., Lykousis, V., Bouloubassi, I., Emeis,
886 K.-C., Kouli, K., Dimiza, M., Rosell-Mele, A., Papanikolaou, M., Katsouras, G., and Nunez,
887 N.: Late Glacial-Holocene climate variability at the south-eastern margin of the Aegean Sea,
888 Mar. Geol., 266, 182-197, 2009b.

889 Triantaphyllou, M.V., Gogou, A, Bouloubassi, I., Dimiza, M, Kouli, K., Rousakis, A.G.,
890 Kotthoff, U., Emeis, K.C., Papanikolaou, M., Athanasiou, M., Parinos, C., Ioakim, C., V. and
891 Lykousis, V.: Evidence for a warm and humid Mid-Holocene episode in the Aegean and
892 northern Levantine Seas (Greece, NE Mediterranean), Regional Environmental Change, 14,
893 1697-1712, 2014.

894 Triantaphyllou, M.V., Gogou, A., Dimiza, M.D., Kostopoulou, S., Parinos, C., Roussakis, G.,
895 Geraga, M., Bouloubassi, I., Fleitmann, D., Zervakis, V., Velaoras, D., Diamantopoulou, A.,
896 Sampataki, A. and Lykousis, V.: Holocene Climate Optimum centennial-scale
897 paleoceanography in the NE Aegean Sea (Mediterranean Sea), Geo-Marine Letters, 36, 51-66,
898 2016.

899 Trigo R.M. and 21 coauthors: Relations between variability in the Mediterranean region and
900 Mid-latitude variability. In: Lionello P, Malanotte-Rizzoli P., Boscolo R., Eds., The
901 Mediterranean Climate: An overview of the main characteristics and issues. Elsevier,
902 Amsterdam, 2006.

903 Tzedakis, P.C.: Seven ambiguities in the Mediterranean palaeoenvironmental narrative,
904 Quaternary Sci. Rev., 26, 2042-2066, 2007.

905   Vannière, B., Power, M.J., Roberts, N., Tinner, W., Carrion, J., Magny, M., Bartlein, P., and

906   Contributors Data: Circum-Mediterranean fire activity and climate changes during the mid

907   Holocene environmental transition (8500-2500 cal yr BP), Holocene, 21, 53-73, 2011.

908   Vannière, B., Magny, M. , Joannin, S. , Simonneau, A. , Wirth, S.B. , Hamann, Y., Chapron,

909   E., Gilli, A., Desmet, M., and Anselmetti, F.S.: Orbital changes, variation in solar activity and

910   increased anthropogenic activities: controls on the Holocene flood frequency in the Lake Ledro

911   area, Northern Italy, Clim. Past, 9, 1193-1209, 2013.

912   Verheyden S., Nader F.H., Cheng H.J., Edwards L.R. and Swennen R.: Paleoclimate

913   reconstruction in the Levant region from the geochemistry of a Holocene stalagmite from the

914   Jeita cave, Lebanon, Quaternary Research, 70, 368-381, 2008.

915   Walczak, I.W., Baldini, J.U.L., Baldini, L.M., Mcdermott, F., Marsden, S., Standish, C.D,

916   Richards, D.A., Andreo, B and Slater J.: Reconstructing high-resolution climate using CT

917   scanning of unsectioned stalagmites: A case study identifying the mid-Holocene onset of the

918   Mediterranean climate in southern Iberia, Quaternary Science Reviews 127, 117-128, 2015.

919   Wilks D. S.: Statistical methods in the atmospheric sciences (Academic Press, San Diego, CA),

920   1995.

921   Wood, S.N. Fast stable restricted maximum likelihood and marginal likelihood estimation of

922   semiparametric generalized linear models. J. of the Royal Statistical Society 73(1), 3-36, 2011.

923   Wu, H., Guiot, J., Brewer, S., and Guo, Z.: Climatic changes in Eurasia and Africa at

924   the Last Glacial Maximum and mid-Holocene: reconstruction from pollen data using inverse

925   vegetation modelling, Clim. Dyn., 29, 211-229, 2007.

926   Zanchetta, G., Borghini, A., Fallick, A.E., Bonadonna, F.P., and Leone, G.: Late Quaternary

927   palaeohydrology of Lake Pergusa (Sicily, southern Italy) as inferred by stable isotopes of

928   lacustrine carbonates, J. Paleolimnol., 38, 227-239, 2007.

929   Zhornyak, L.V., Zanchetta, G., Drysdale, R.N., Hellstrom, J.C., Isola, I., Regattieri, E., Piccini,

930   L., Baneschi, I., and Couchoud, I.: Stratigraphic evidence for a "pluvial phase" between ca.

931   8200-7100 ka from Renella cave (Central Italy), Quat. Sci. Rev., 30, 409-417, 2011.
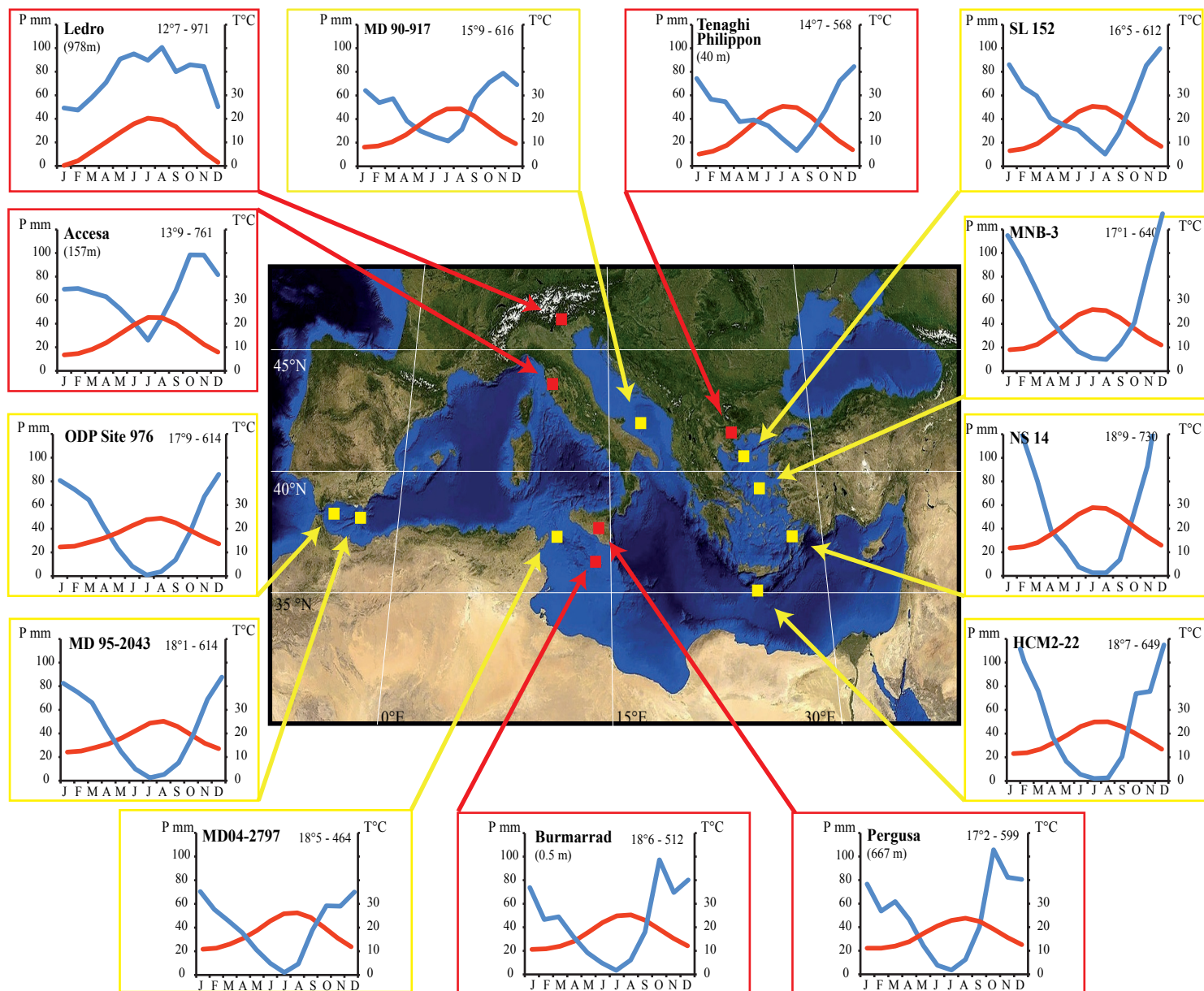
Figure 1: Locations of terrestrial (red) and marine (yellow) pollen records.
Ombrothermic diagrams are calculated with the NewLoclim software, which provides estimates of average climatic conditions at locations for which no observations are available (ex.: marine pollen cores).

Annual precipitation 8000-6000 cal yrs BP
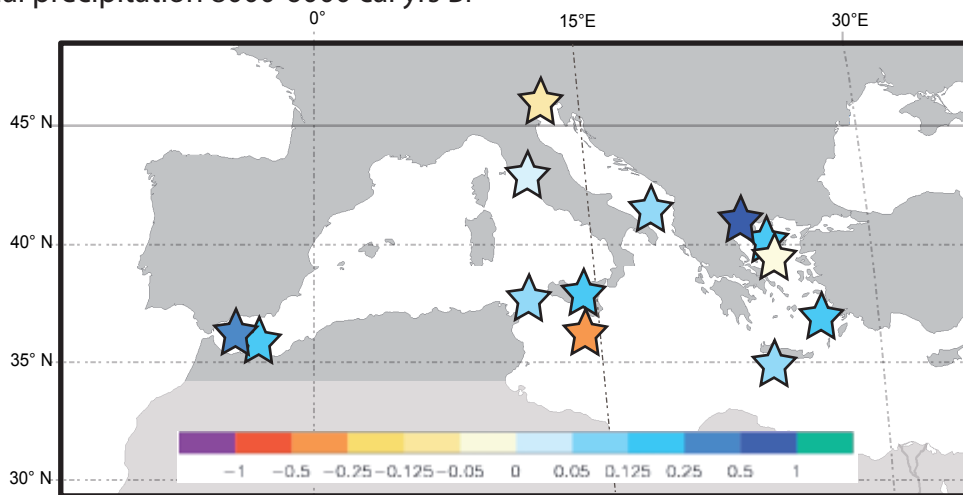
Winter precipitation 8000-6000 cal yrs BP
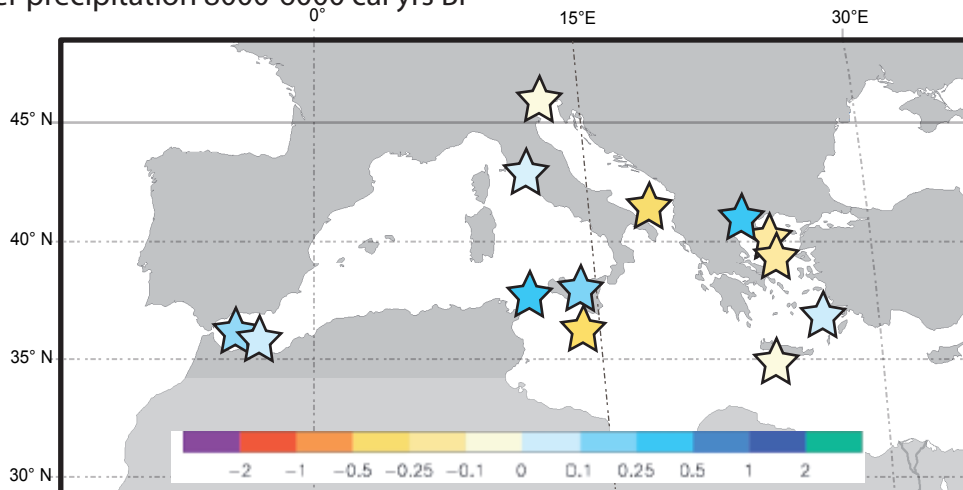
Summer precipitation 8000-6000 cal yrs BP
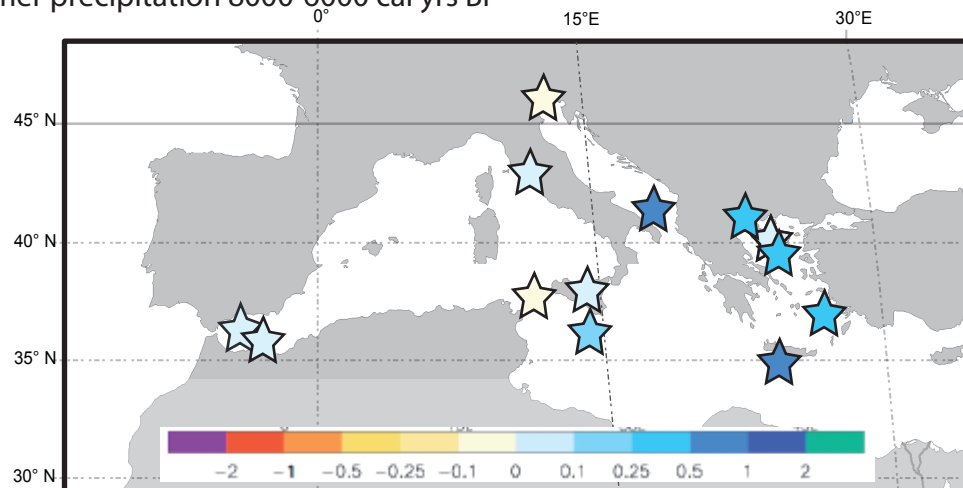
Figure 2a: 8000-6000 cal years BP
 Pollen-inferred climate estimates as performed with the Modern Analogues Technique: annual precipitation, winter precipitation (winter = sum of December, January and February precipitation) and summer precipitation (summer = sum of June, July and August precipitation). Changes in climate are expressed as differences with respect to the modern values (anomalies, mm/day), which are derived from the ombrothermic diagrams (cf Fig. 1). Climate values reconstructed during the 8000-6000 cal yrs BP have been averaged (stars).

Annual precipitation 4000-2000 cal yrs BP
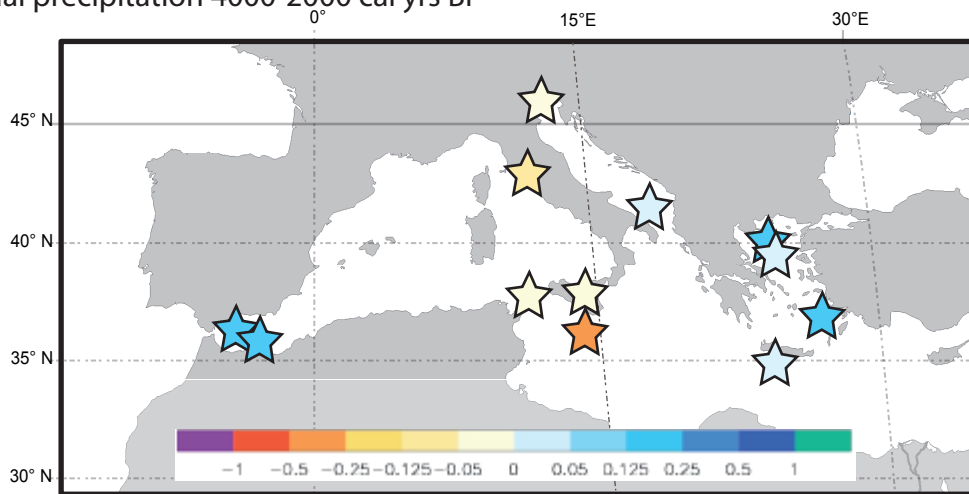
Winter precipitation 4000-2000 cal yrs BP
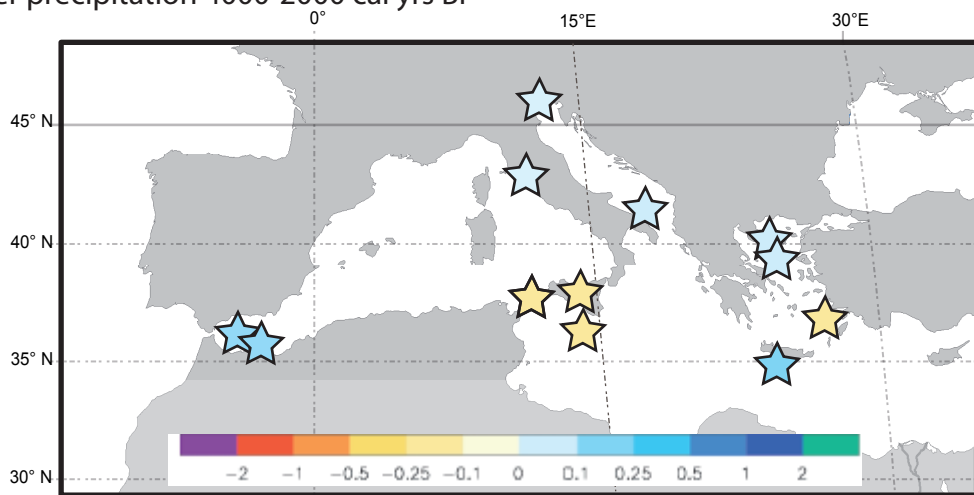
Summer precipitation 4000-2000 cal yrs BP
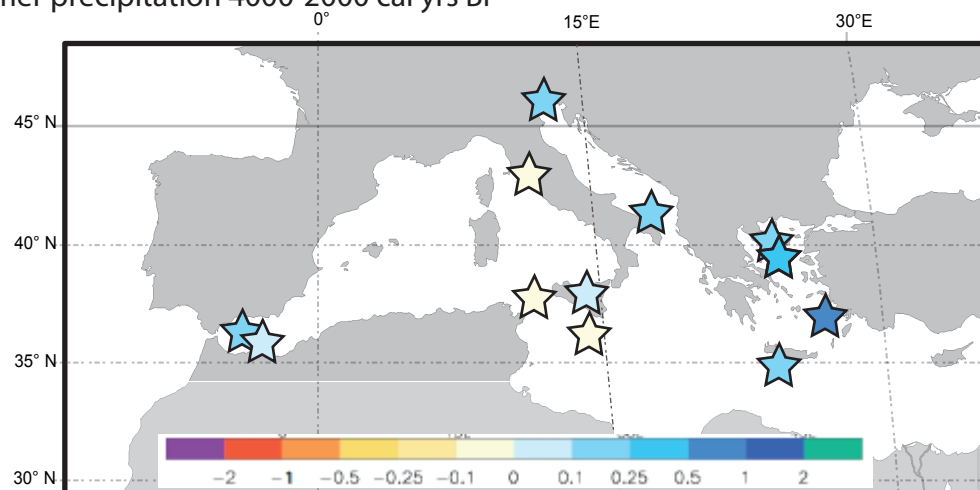
Figure 2b: 4000-2000 cal yrs BP
Pollen-inferred climate estimates as performed with the Modern Analogues Technique: annual precipitation, winter precipitation (winter = sum of December, January and February precipitation) and summer precipitation (summer = sum of June, July and August precipitation). Changes in climate are expressed as differences with respect to the modern values (anomalies, mm/day), which are derived from the ombrothermic diagrams (cf Fig. 1). Climate values reconstructed during the 4000-2000 cal yrs BP have been averaged (stars).
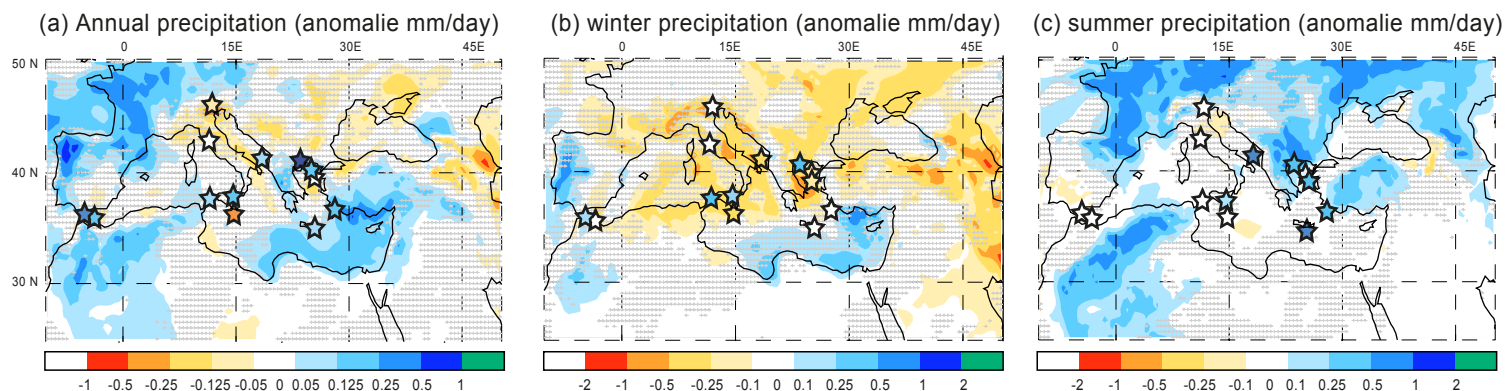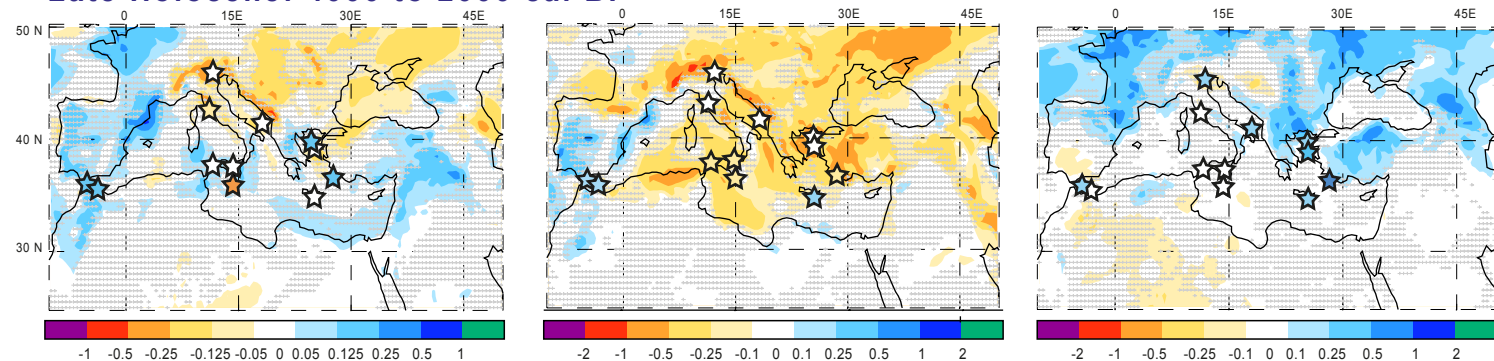
Figure 3: Data-model comparison for mid and late Holocene precipitation, expressed in anomaly (mm/day)
Simulations are based on a regional model (Brayshaw et al., 2010): standard model HadAM3 coupled to HadSM3
and HadRM3 (high-resolution regional model). The hatched areas indicate areas where the changes are not significant (threshold used here 70%).
Pollen-inferred climate estimates (stars) are the same as in Fig.2: annual precipitation, winter precipitation and summer precipitation .
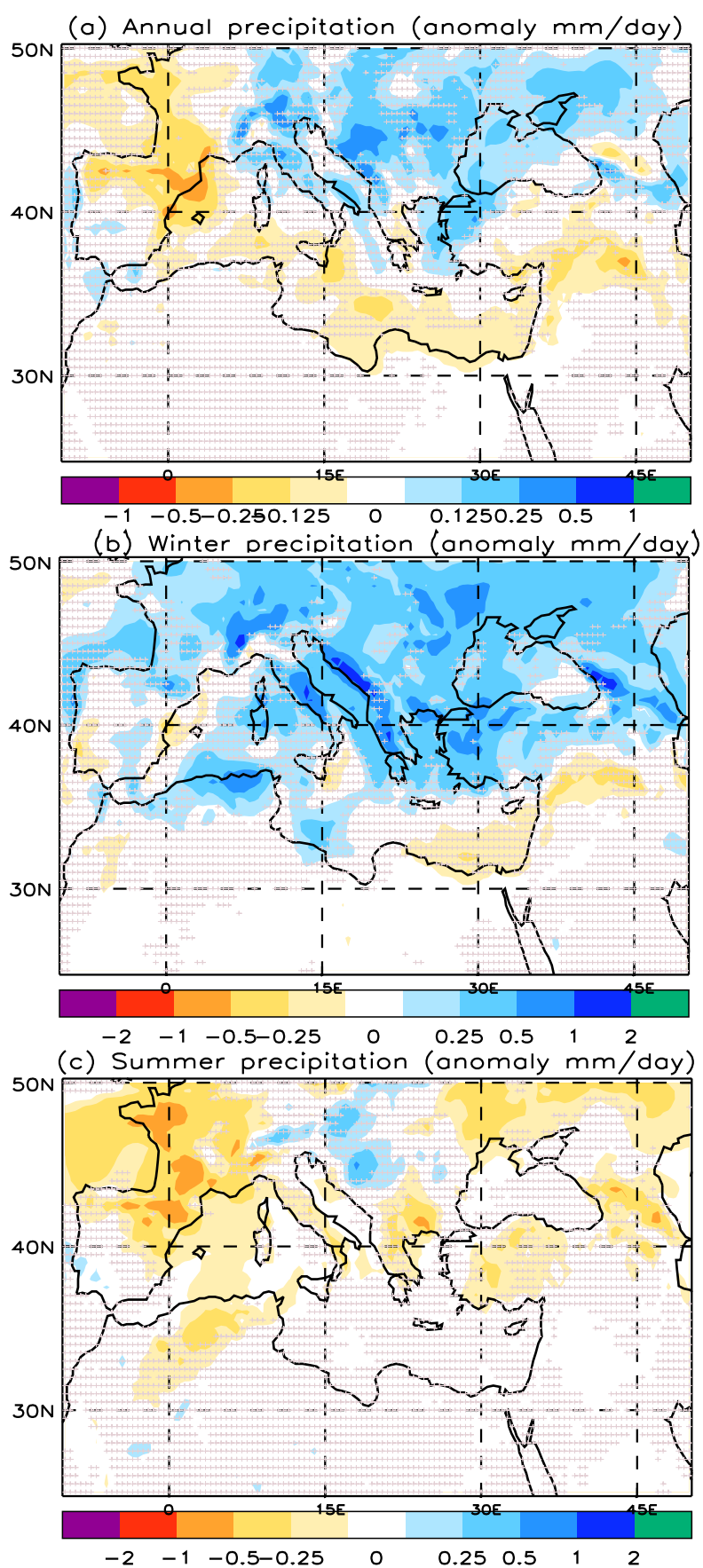
Figure 4: Model simulation showing Present day minus Preindustrial precipitation anomalies
(hatching at 70%/statistical significance over the insignificant regions)

Terrestrial pollen records

	Longit.	Latitude	Elev. (m a.s.l)	Temporal resolution	References (non- exhaustive)
Ledro (North Italy)	10°76'E	45°87'N	652	8000-6000: 71 4000-2000: 60 10966-10: 66	Joannin et al. (2013), Magny et al. (2009, 2012a), Vannière et al. (2013), Peyron et al. (2013)
Accesa (Central Italy)	10°53'E	42°59'N	157	8000-6000: 90 4000-2000 : 133 11029-100: 97	Drescher-Schneider et al. (2007), Magny et al. (2007, 2013), Colombaroli et al. (2008), Sadori et al. (2011), Vannière et al. (2011), Peyron et al. (2011, 2013)
Trifoglietti (Southern Italy)	16°01'E	39°33'N	1048	8000-6000: 95 4000-2000: 86 9967-14: 73	Joannin et al. (2012), Peyron et al. (2013)
Pergusa (Sicily)	14°18'E	37°31'N	667	8000-6000: 166 4000-2000: 90 12749-53: 154	Sadori and Narcisi (2001); Sadori et al. (2008, 2011, 2013, 2016b); Magny et al. (2011, 2013)
Tenaghi Philippon (Greece)	24°13.4'E	40°58.4'N	40	8000-6000: 64 4000-2000: no 10369-6371:53	Pross et al. (2009, 2015), Peyron et al. (2011), Schemmel et al., (2016)
Burmarrad (Malta)	14°25'E	35°56'N	0.5	8000-6000: 400 4000-2000: 285 6904-1730: 110	Djamali et al. (2013), Gambin et al., (2016)

Marine pollen records

	Longit.	Latitude	Water-depth	Temporal resolution	References
ODP 976 (Alboran Sea)	4°18'W	36°12' N	1108	8000-6000: 142 4000-2000: 181 10903-132: 129	Combourieu-Nebout et al. (1999, 2002, 2009) ; Dormoy et al., (2009)
MD95-2043 (Alboran Sea)	2°37'W	36°9'N	1841	8000-6000: 111 4000-2000: 142 10952-1279: 106	Fletcher and Sánchez Goñi (2008); Fletcher et al., (2010)
MD90-917 (Adriatic Sea)	17°37'E	41°97'N	845	8000-6000: 90 4000-2000: 333 10495-2641: 122	Combourieu-Nebout et al. (2013)
MD04-2797 (Siculo-Tunisian strait)	11°40'E	36°57'N	771	8000-6000: 111 4000-2000: 666 10985-2215: 127	Desprat et al. (2013)
SL152 (North Aegean Sea)	24°36' E	40°19' N	978	8000-6000: 60 4000-2000: 95 9999-0: 76	Kotthoff et al. (2008, 2011), Dormoy et al. (2009).
NS14 (South Aegean Sea)	27°02'E	36°38'N	505	8000-6000: 80 4000-2000: 333 9988-2570: 107	Kouli et al. (2012) ; Gogou et al. (2007); Triantaphyllou et al. (2009a, b)
HCM2/22 (South Crete)	24°53'E	34°34 N	2211	8000-6000: 181 4000-2000: 333 8091-2390: 247	Ioakim et.al. (2009) ; Kouli et al, (2012) ; Triantaphyllou et al. (2014)

MNB-3 (North Aegean Sea)	25°00'E	39°15'N	800	8000-6000: 153	Geraga et al. (2010) ; Kouli et al.,
				4000-2000: 166	(2012) ; Triantaphyllou et al,
				8209-2273: 138	(2014)

Table 1: Metadata for the terrestrial and marine pollen records evaluated. The temporal resolution is calculated for the two periods (8000-6000 and 4000-2000) and for the entire record.